Currents, Eddies, and a "Fish Story" IN THE SOUTHWESTERN JAPAN/EAST SEA

BY D. RANDOLPH WATTS, MARK WIMBUSH, KAREN L. TRACEY, WILLIAM J. TEAGUE, JAE-HUN PARK, DOUGLAS A. MITCHELL, JONG-HWAN YOON, MOON-SIK SUK, AND KYUNG-IL CHANG

GOALS AND APPROACH

As part of the Japan/East Sea (JES) initiative supported by the U.S. Office of Naval Research, we conducted an observational experiment to understand the physics of the mesoscale circulation in the Ulleung Basin, located in the southwestern corner of the JES. The current passing through the Korea Strait divides upon entering the JES, with portions of the current flowing along the Korean and Japanese coasts. The variability of these currents is especially energetic in our study region. Our objectives were to measure the time-varying currents in the upper and deep levels of the JES. We relate the population density of vertically migrating fish or squid to the time-varying locations of fronts.

We moored a two-dimensional array of pressure-gauge-equipped inverted echo sounders (PIES) and deep-recording current meters for 24 months starting June 1999. Figure 1 shows the study region, which spanned roughly a 250-km square between the Republic of Korea and Japan. The inverted echo sounder is a bottom-moored instrument that measures the time required for an acoustic pulse to travel from the seafloor to the sea surface and back. Travel-time variations arise primarily from temperature changes in the overlying water column caused by meandering fronts and eddies. The PIES array was used to map the temperature field at a suite of depth levels and the dynamic method was used to calculate profiles of geostrophic current. Bottom pressure and deep current meters moored 25 m above the seafloor were used together to map the deep circulation.

Almost serendipitously, our findings about mesoscale variability linked it both to longer- and to shorter-period variability (i.e., from interannual down to periods of 10 days to a few hours). This paper treats the long-period processes ranging from interannual periods down to a few days. The companion article by Park et al. (this issue) treats the short-period processes, demonstrating how they are related to the larger-scale circulation, and suggests improvements for using satellite altimeter data in marginal seas like the JES. For a comprehensive review of the circulation in the region, see Chang et al. (2004).

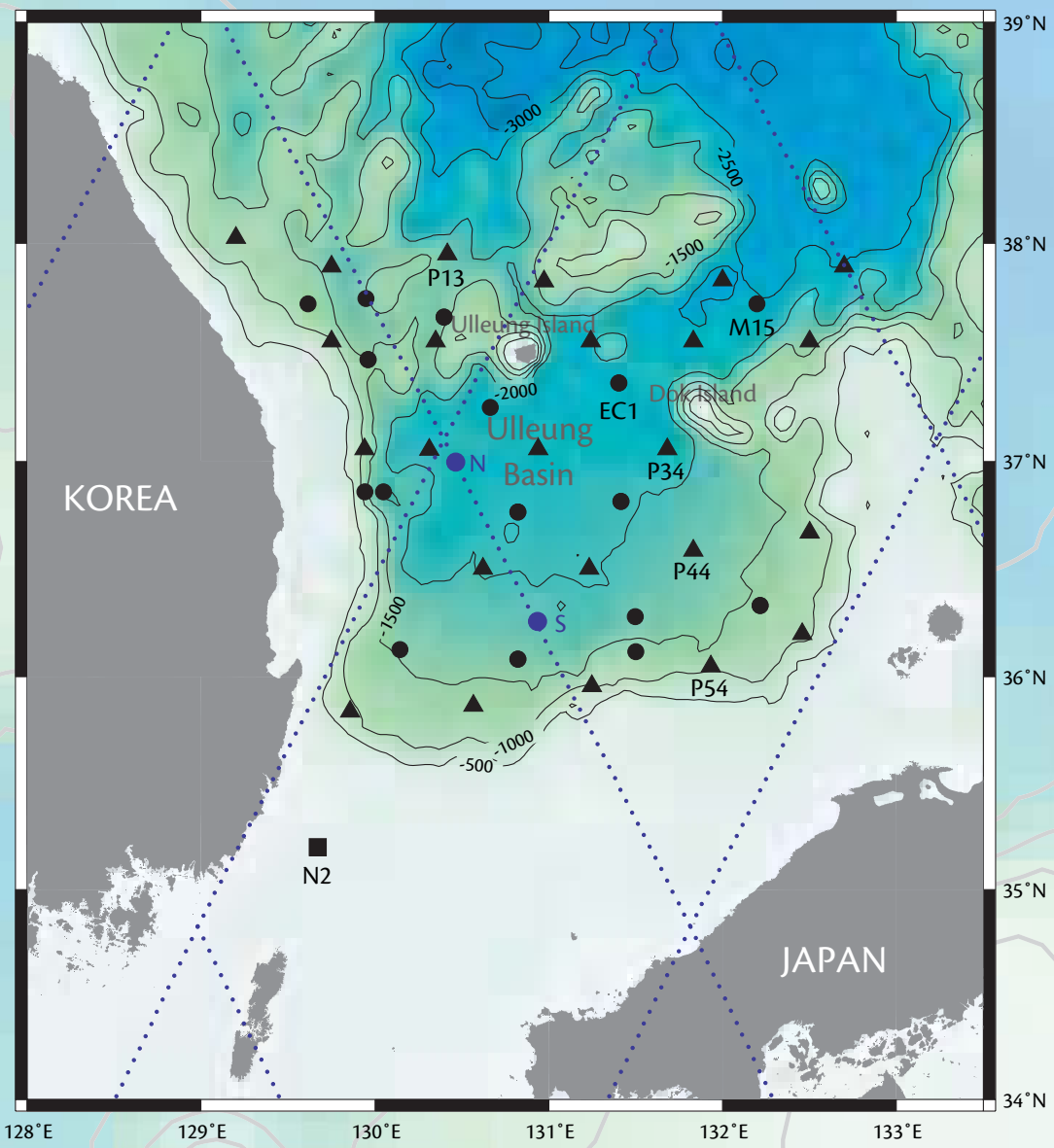

Figure 1. Pressure-gauge-equipped inverted echo sounders (PIES, triangles) and recording current meters (circles) were deployed between June 1999 and June 2001 to measure the upper and deep circulation in the Ulleung Basin, southwestern region of the Japan/East Sea (JES) between Korea and Japan. The square indicates one (site N2) of several Acoustic Doppler Current Profiler moorings in the Korea/Tsushima Strait occupied between May 1999 and June 2000. TOPEX/Poseidon (T/P) ground tracks are shown by the dotted blue lines. Two large blue circles labeled N and S indicate locations where spectra were computed for geostrophic currents estimated separately by the T/P and mapped PIES data. Data from labeled sites are discussed in the text. Bathymetry is color shaded and contoured at 500-m intervals.

CURRENT RECORDS SPANNING NINE YEARS TO ONE HOUR

To knit this article together with that of Park et al. (this issue), we have constructed a composite record of regional currents from different sources: satellite altimetry for decadal to monthly time scales, the moored PIES array for two-year to five-day time scales, and moored current meters and an Acoustic Doppler Current Profiler (ADCP) for monthly to hourly time scales. In combination, the time variability displayed by these current records can be summarized according to how much energy is associated with processes of different frequency—the "current spectrum," as illustrated in Figure 2.

The current spectrum pieced together from these several sources spans an exceptionally large range of periods, from nine years to two hours. It exhibits a classic "red" spectrum, with higher energies at lower frequencies. The bottom panel in Figure 2 is a variance-preserving plot in which the area under the curve is proportional to the energy, illustrating that by far most of the kinetic energy is in the band of periods from 50 to 500 days. The strong tidal currents through the Korea Strait account for the large (green) peaks at diurnal and semidiurnal periods. Other high-frequency processes require a separate plot with expanded vertical scale (inset) to see their kinetic energies. The current spectra are repeated in a log-log plot in the top panel of Figure 2 to help interpret the enormous range of observed energies. The overall spectral trend has a slope of -5/3, but with significant structural departures. The processes and labeled peaks and valleys will be discussed, starting with the longest periods.

> Our two-year mappings of the upper and deep current systems found more complicated variable circulation patterns than the traditional "three-currents paradigm," and the patterns do not repeat seasonally.

The geostrophic surface current can be calculated from the slope of sea surface height (SSH) measured by satellite altimeter (Teague et al., 2004). The component of current perpendicular to a TOPEX/Poseidon (T/P) ground track was determined at two representative sites in Figure 1, producing records of nine-years duration. Their spectra are the purple lines in Figure 2, analyzed for periods between nine years and 20 days, however, these spectral estimates fall artificially at periods shorter than 50 days because of smoothing of the altimeter product. The spectral energies increase with decreasing frequency, even out to the longest-estimated periods (3240 days)—in accord with strong interannual and climate variability in the Pacific and in the atmosphere at decadal and longer time scales. Frequencies near the label "EN" (1280 days) would correspond to El Niño processes, but surprisingly no local maximum energy appears with a 3–6 year period in these current spectra. Moreover, at point "A" the annual cycle of variability produces only a weak peak in the current spectra, and appears merely to be part of the 50-to-500-day mesoscale energetic band.

During our two-year study, geostrophic surface currents were mapped throughout the Ulleung Basin using data

D. Randolph Watts *(rwatts@gso.uri.edu) is Professor, Graduate School of Oceanography, University of Rhode Island, Narragansett, RI, USA.* **Mark Wimbush** *is Professor, Graduate School of Oceanography, University of Rhode Island, Narragansett, RI, USA.* **Karen L. Tracey** *is Research Specialist, Graduate School of Oceanography, University of Rhode Island, Narragansett, RI, USA.* **William J. Teague** *is Section Head, Meso- and Finescale Ocean Physics Section, Naval Research Laboratory, Stennis Space Center, MS, USA.* **Jae-Hun Park** *is Research Scientist, Graduate School of Oceanography, University of Rhode Island, Narragansett, RI, USA.* **Douglas A. Mitchell** *is Senior Research Engineer, Exxon Mobil Upstream Research Company, Houston, TX, USA.* **Jong-Hwan Yoon** *is Professor, Research Institute for Applied Mechanics, Kyushu University, Japan.* **Moon-Sik Suk** *is Principal Research Scientist, Korea Ocean Research and Development Institute, Ansan, Republic of Korea.* **Kyung-Il Chang** *is Associate Professor, School of Earth and Environmental Sciences, Seoul National University, Seoul, Republic of Korea.*

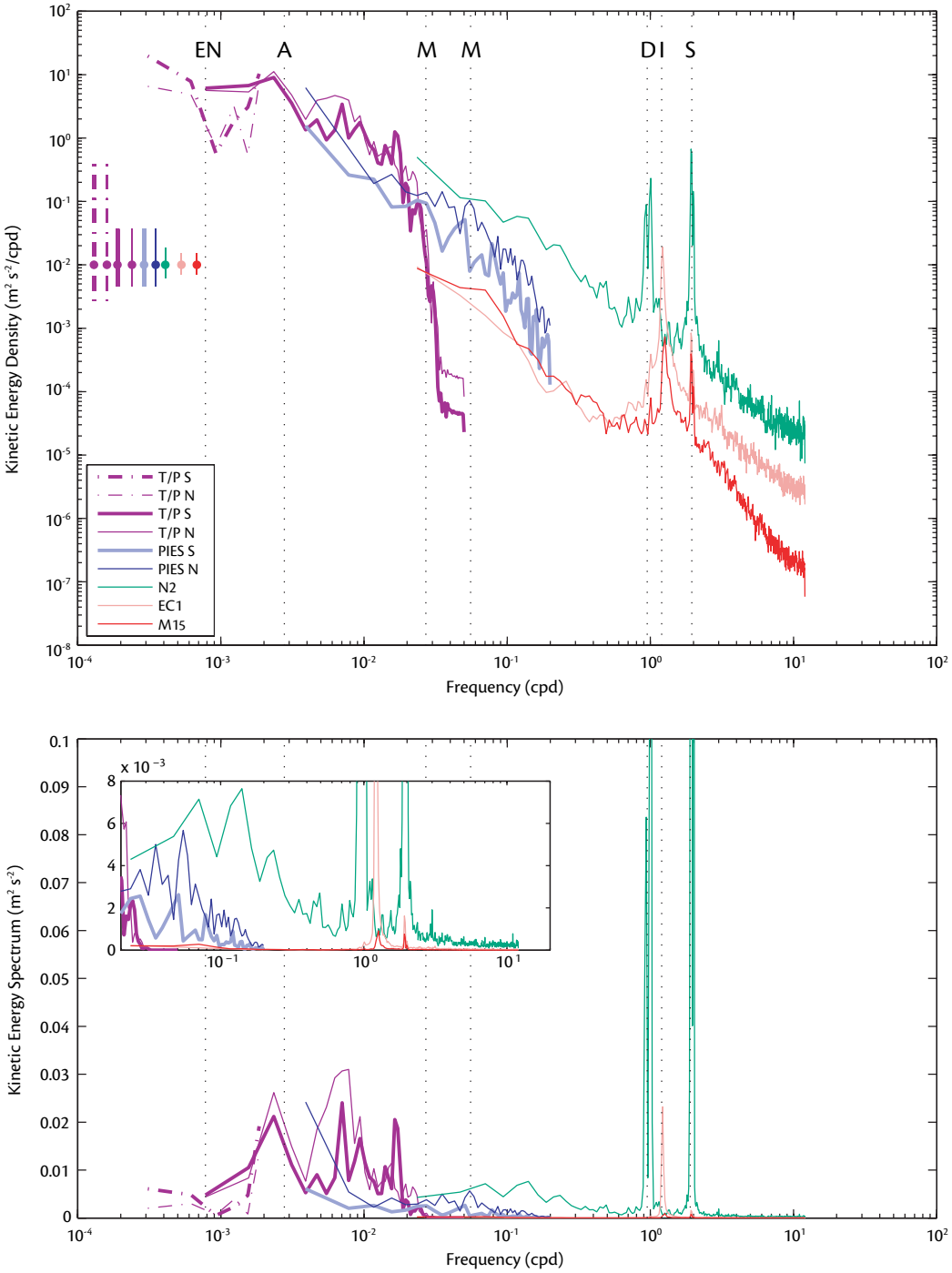

Figure 2. The amount of kinetic energy associated with processes at different frequencies is illustrated by their spectra calculated from measurements by a variety of instrumentation. A peak in the spectrum indicates more energy at its corresponding frequency. For example, the peak labeled S arises from semidiurnal tidal currents. The spectra are shown for the NE/SW component of flow, which is perpendicular to the satellite altimeter ground track shown in Figure 1. Geostrophic surface currents were derived from satellite altimetric measurements as well as from the mapped PIES data at the same two locations (marked by the blue circles labeled N, S in Figure 1). Their corresponding spectra are shown by the purple and blues lines, respectively. The solid and dashed purple lines are spectral estimates generated from the same data sets, but averaged using different segment lengths. To resolve the longest periods (dashed), fewer segments are averaged, resulting in broader confidence intervals. Measured currents at variable depths are shown for the remaining sites. Error bars show the 95 percent confidence limits. The key in the upper frame applies to all frames and the instrument locations are labeled in Figure 1. (Top) Auto-spectral density. (Bottom) Variance-preserving spectra. Inset is an enlargement of the higher-frequency signals.

from the PIES array. Choosing the same two locations along the T/P track and the same current components as for the altimeter, we illustrate in Figure 2 the current spectra (two blue lines) in the middle range of periods between 256 days and 5 days. The hourly PIES records were 120-hour low-pass filtered for these geostrophic current calculations. The mesoscale processes with periods between semi-weekly and sub-annual were roughly half as energetic during our two-year study (6/1999–6/2001) as during the nine years (1993–2002). To check for bias, we analyzed the altimeter SSH record for

just the same two years and found spectral levels (not shown) consistent with those from the PIES records. Hence, these two years were somewhat less energetic than the nine-year average. This band of mesoscale eddy processes continues the general spectral slope of -5/3. Weak peaks like those marked "M" (at 37 and 18 days) are present in other current spectra from the Ulleung Basin, but different sites generally exhibit somewhat different mesoscale peak frequencies.

Three additional current spectra in Figure 2 exemplify higher-frequency processes with periods between 43 days and two hours from directly measured hourly records of currents. The companion article by Park et al. (this issue) treats these short-period processes. The green curve shows the spectrum of along-channel, depth-averaged (30–80 m) currents from an ADCP moored within the Korea Strait (Teague et al., this issue). The highly energetic peaks "D" and "S" are from the strong diurnal and semi-diurnal barotropic tidal currents. These tidal currents are driven by relatively large tidal-height differences through the Korea Strait, because the range of tides inside the JES is exceptionally small. Throughout the band of periods from 43 days to five days, the kinetic-energy levels within the Korea Strait are approximately four times higher than for surface currents within the JES. The relatively strong currents through the Korea Strait at mesoscale frequencies arise because of substantial along-channel pressure gradients, produced presumably by energetic mesoscale eddies in the East China Sea outside the Korea Strait. Lyu and Kim (2005) showed that pressure-gradient forces along the Korea Strait play the dominant role governing transport variations of 1–2 Sv at monthly to interannual periods.

The most directly comparable hourly sampled current record available to us is the uppermost current meter on the KORDI mooring, EC1, at 400-m nominal depth in approximately 2400-m water depth in the channel between Ulleung and Dok Islands (Chang et al., 2002). Its spectral levels in the 43-day to five-day band (pink curve) are lower by a factor of about five than the blue curves in Figure 2 for surface currents, because the 400-m instrument depth lies below the main thermocline. Hence, currents at this depth include only a small fraction of the upper baroclinic currents, plus of course the deep reference barotropic currents. An example of the deep near-bottom current spectra is shown by the red line on Figure 2 (site M15 at 2425 m depth). In comparison to the 400-m level, the deep kinetic-energy levels are similar for periods longer than two days, but are less than half as great at daily and higher frequencies.

The tidal currents within the JES, as exemplified by both the EC1 and M15 sites, are much weaker than the barotropic tidal currents through the Korea Strait. They are associated mainly with internal baroclinic tides, and the energy at "D" is much lower than at "S." Both exhibit relatively strong inertial peaks, "I." This is a typical pattern for current spectra poleward of 30 degrees, because the stratified water column only supports free internal waves between the inertial period and buoyancy period. A noticeable spectral gap exists between this internal-wave band and the mesoscale band, exhibited as a decrease in spectral density by about a factor of ten for periods one day to ten days. The spectrum from the Korea Strait (green curve) is an exception in this respect also, with energetic current fluctuations in periods two days to ten days. The Korea Strait currents include a strong barotropic component in response to atmospheric forcing, and hence fill that spectral gap (Lyu et al., 2002; Park and Watts, 2005; Park et al., this issue; Teague et al., this issue).

CIRCULATION FEATURES AND PATTERNS IN THE JES

Perhaps it is not surprising that, based now on sufficient observations (discussed by Mitchell et al., 2005a), the currents and circulation in the southwestern JES *differ* from the former paradigm in which three currents branch out from the Korea Strait in seasonally repeating paths. Nevertheless, we reconfirmed several persistent and/or recurrent features of the upper circulation. In fact, all the features summarized in Figures 3 and 4, except the Dok Cold Eddy, had been identified previously, and their recurrence and persistence had apparently contributed to the erroneous concept that the circulation varied in a regular seasonal progression of patterns (Mitchell et al., 2005b).

The upper circulation and thermocline depth were mapped at daily intervals by the PIES array (Mitchell et al., 2005a). The measurements by the bottom pressure sensors and deep current meters were used in combination to map the deep absolute currents (Teague et al, 2005). Because of the intense bottom fishing and crabbing in the Ulleung Basin at depths as great as 2000 m, the instruments were moored close to the

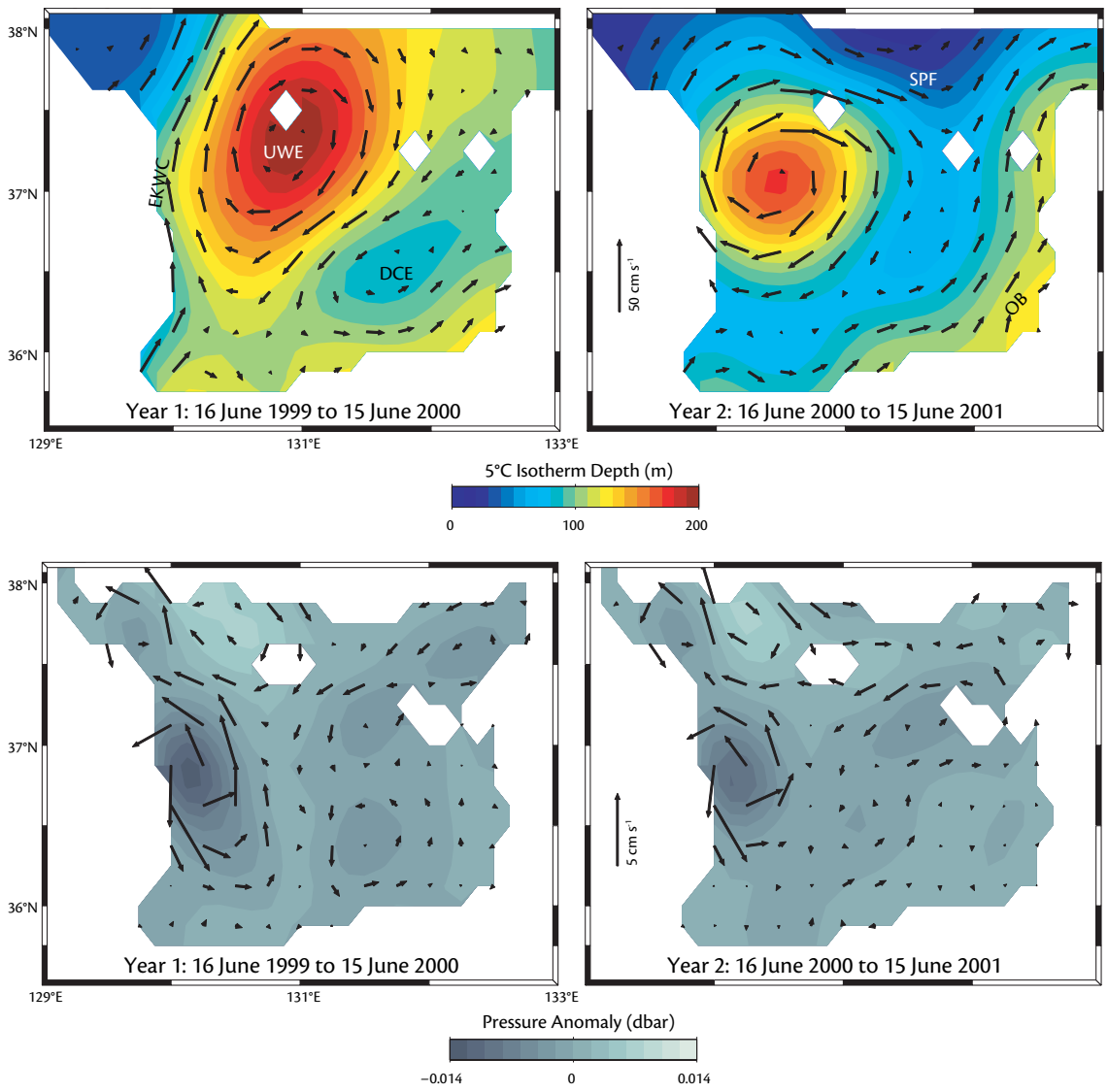

Figure 3. (Upper) Annual mean maps of the 5°C isotherm depth and geostrophic surface currents relative to 1000 dbar are shown for (Left) Year 1 and (Right) Year 2. Persistent current features discussed within the text are indicated in the two frames: East Korean Warm Current (EKWC), Ulleung Warm Eddy (UWE), Dok Cold Eddy (DCE), Offshore Branch (OB), and the Subpolar Front (SPF). During the first year, the UWE was strongly developed and the Ulleung Basin was generally warm throughout. In contrast, during the second year, the UWE was smaller and the SPF shifted south of 38°N; as a result the basin was colder. (Lower) Annual mean deep dynamic pressure maps and deep absolute currents. Unlike the upper fields, these deep fields are similar during the two years.

bottom to avoid losses. Despite these precautions, we found evidence that several of the PIESs were snagged and dragged short distances during the mooring period.

Figure 3 (upper panels) shows the annual averages of the circulation in the Ulleung Basin, mapping the surface current vectors and the thermocline depth (5°C isotherm depth) for two years. The upper circulation features (Figure 3) include: a western boundary current along the Korean coast called the East Korea Warm Current (EKWC); the Subpolar Front (SPF) that flows eastward as a free jet approximately along 38°N and meanders through more than a degree of latitude; a current that hugs the southeastern shelf break called the Offshore Branch (OB);[1] the Ulleung Warm Eddy (UWE), a strong anticyclonic warm eddy that was almost always present near or encircling Ulleung Island (Figure 1); and the Dok Cold Eddy (DCE), a cyclonic cold eddy that was usually present in the southeastern Ulleung Basin with 0.1 m s^{-1} to 0.3 m s^{-1} surface currents. The DCE forms when a steep trough of the SPF pinches off a cold eddy. These cold eddies remain stationary or propagate south-

[1] Southeast of our observations, nearer yet to the Japanese coast along the shallow shelf, flows the "Nearshore Branch." This branch, together with the OB and EKWC, constitute the three traditional branches that originate from the Korea Strait.

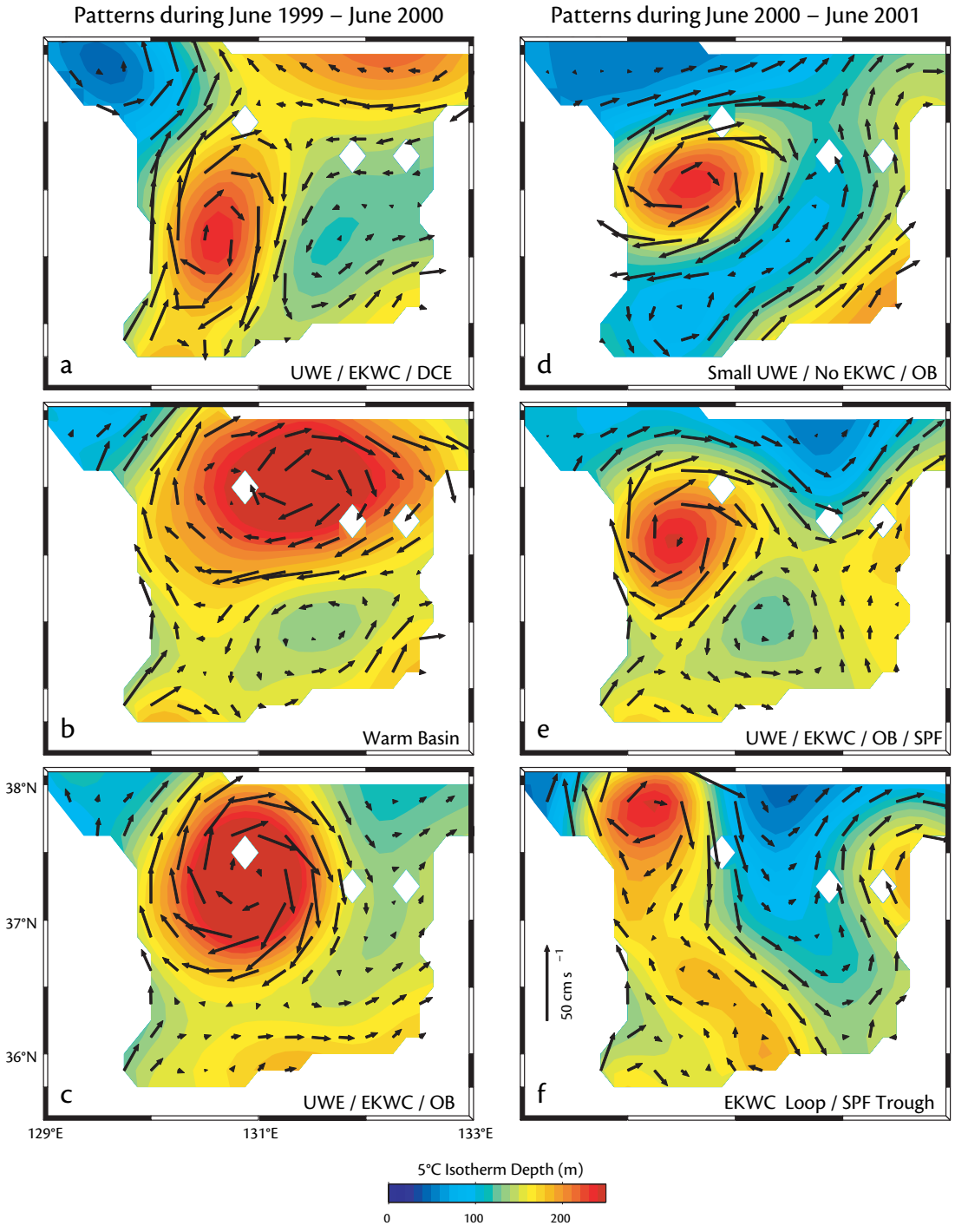

Figure 4. Mesoscale variability of the upper circulation in the JES was observed by the PIES array. Six quasi-stable patterns observed during the experiment, grouped by year, illustrate the variability of the paths of the EKWC, OB, and SPF as well as the evolution of the UWE and DCE on intra-annual time scales. Mean maps are shown of the 5°C isotherm depth and surface currents for selected intervals varying in length between six weeks and five months. The significance of each panel is discussed in the text.

westward to the Korean shelf near 36°N.

The annual mean deep circulation is shown in Figure 3 (lower panels). Because density profiles in the JES are nearly homogenous below the pycnocline, vertical shear is negligible at depth. Thus, Figure 3 illustrates the circulation patterns below 1000 m. Teague et al. (2005) discuss this deep circulation. There is a weak mean (< 1 cm s^{-1}) cyclonic flow in the east-central part of the basin and a concentrated cyclonic eddy (~5 cm s^{-1}) near the western boundary. There is generally inflow (~2 cm s^{-1}) through the only deep channel entering the basin between Ulleung and Dok Islands, suggesting upwelling and entrainment into the upper-level flow within the otherwise closed

deep basin. However, it is possible there is a localized outflow within this channel that was not resolved by our array. The outflow shown in the northwestern portion of these maps should be interpreted together with the bathymetric chart in Figure 1, which indicates that this flow occurs at much shallower depths and passes over the Korea Plateau.

Figure 3 also emphasizes that the upper circulation changes from one year to another (Park and Watts, 2006). From June 1999 to June 2000 (Year 1) the EKWC on average protruded north of 38.25°N. The circulation around the UWE was strong, and the DCE had only weak cyclonic mean circulation. Our observations exhibited only the outer portion of the OB flowing along the southeastern shelf break and onto the Oki Spur. From June 2000 to June 2001 (Year 2), the annual average showed a weaker EKWC that turned eastward offshore to feed the SPF, which meandered during this year along approximately 37.5°N. Mitchell et al. (2005a) concluded that the EKWC was absent from 11 June to 5 November 2000, and confirmed this absence of the EKWC against bimonthly hydrographic surveys by the National Fisheries Research and Development Institute of Korea on six transects that extended from the coast across the shelf and into the Ulleung Basin. This second year exhibited in the mean a much contracted form of the UWE and a steep cold trough of the SPF dipped far southward into the Ulleung Basin near 131.7°E. A strong OB flowed along the southeastern shelf break and turned northward between 132°E and 132.5°E following the Oki Spur. Interestingly, the disappearance and reestablishment of the EKWC was not directly linked to variations in the total transport through the Korea Strait. Mitchell et al. (2005a) note that the inflow diverted into either the Nearshore Branch or the OB (or both)—and we have just noted the increased strength of the OB.

During the two-year experiment, a given circulation pattern typically persisted for 2–4 months and then made a transition within a few weeks to a different pattern, as summarized by Mitchell et al. (2005a, 2005b). Six circulation patterns are illustrated in Figure 4, each showing a time-average field of 5°C isotherm depth and grid of surface current vectors that represents approximately a four-month interval. The observed circulation patterns for the first and second years are shown in the left and right columns, respectively, and are summarized below.

Panel (a) represents 15 June to 30 September 1999 in which a strong EKWC flows northward along the Korean coast and bifurcates. Part of the flow continues north of 38.25°N, and part loops back southward around an elongated UWE and subsequently turns northeastward around the weak DCE to join the OB. During this interval, the volume transport through the Korea Strait reached its peak value during our study.

Panel (b) represents 1 October 1999 to 1 February 2000 in which the Ulleung Basin was unusually warm. The UWE had inflated to cover most of the basin, the SPF had shifted northward beyond this study region, and the DCE was weak.

Panel (c) represents 2 February to 10 June 2000 in which the UWE was particularly strong, maintaining its size around and south of Ulleung Island. The EKWC and OB were both well developed, and the SPF occasionally steepened its trough far into the basin.

Panel (d) represents 17 June to 5 November 2000 in which the EKWC was absent and the UWE rapidly weakened and remained weak. A trough of the SPF dipped repeatedly into the basin, sometimes pinching off a DCE. The OB was greatest during this period while the EKWC was absent.

Panel (e) represents 29 November 2000 to 21 March 2001 in which the EKWC reestablished and the relatively small UWE began to regrow. The SPF meandered along approximately 37.8°N, and the DCE remained relatively stationary and weak during this interval.

Serendipitously, acoustic echoes from vertically migrating fish or squid revealed high population density in warm waters near fronts.

Panel (f) represents 16 April to 21 June 2000, characterized by the EKWC again looping north of 38.25°N. The SPF extended a long broad cold meander trough into the basin.

Although the circulation varies greatly from one year to the next, it can also change substantially from one month to

another. We observed that the circulation patterns may persist for a few months and then change within a few weeks. Although historically the paradigm has suggested seasonally repeating paths for the currents and fronts in the JES, the circulation patterns that we observed for 1999–2001 should not be categorized as "seasonal." Knowledge of the varying circulation has a number of practical applications, such as guiding fishing practices regarding the true location of fronts.

ACOUSTIC REFLECTIONS OFF DIURNALLY MIGRATING FISH OR SQUID

The acoustic signals important to our investigations are the ones that reflect off the sea surface. However, the desired signal may be obscured by other processes. For example, nearby topographic features can reflect the acoustic signals such that they arrive back to the instruments earlier than anticipated. Typhoons and storms passing through an array can generate air bubbles and surface waves that can cause echoes to return later than anticipated.

In the JES, occasional acoustic signals were received earlier than anticipated, and they "migrated" vertically in synchrony with the light cycle and to a depth that coincided with the base of the thermocline. Early echoes returning from as much as 250 m below the surface occurred during the daylight hours, whereas they returned from near surface during the nighttime (Figure 5, bottom panel). The phasing of this pattern indicates biological activity, rather than a physical process. Diel vertical migration is well documented for zooplankton and predators that follow them as a food source. The bottom panel of Figure 5 shows each acoustic ping received by a PIES during a seven-day period shortly after the instrument was deployed. Our desired oceanic signals appear as the broken line of points clustered at the sea surface. The shading each day highlights the interval from 1900 to 0400 local time, which roughly corresponds to nighttime in the midsummer JES.

The upper panels in Figure 5 show the temporal variation of the early echoes for the entire two years at four representative sites. Some instruments, such as P54, received many early returns throughout the two-year period. These sites were typically located along the Japan and Korean shelf breaks. Other sites, such as P34, showed considerable biological activity during the first year, but very little during the second year. (The abrupt cutoff below 220 m at site P34 is an artifact of the instrument preparation intended to lock out early echoes.) Site P44 was unique in that virtually no biological activity occurred during the whole observational period. At all sites, the maximum depth of the early returns changed over time in concert with depth variations of the permanent thermocline. For example, at P13 the echo reflection depth was more than 50 m shallower in spring 2000 than in either fall 1999 or summer 2001.

For each PIES, we calculated the percentage of early echoes that occurred in five-day segments throughout the experiment. The percentages were separated into three categories of biological activity: low (< 5 percent early echoes), medium (5–15 percent), and high (> 15 percent) concentrations. Relationships between biological activity and ocean circulation were revealed by superimposing the percentages on the maps of the 5°C isotherm depth averaged over the corresponding five days. A subset of these maps is shown at 30-day intervals in Figure 6. They reveal high concentrations of organisms in the warm-water regimes, particularly along edges near fronts, whereas the concentrations tend to be low in the cold-water regions. This relationship is particularly apparent when a comparison is made between the maps for Year 1 (upper three rows) and those for Year 2 (lower three rows). The abundance of animals within the basin dropped markedly in Year 2, when the basin was cooled by the meandering Subpolar Front. High concentrations nearly always occurred in the Ulleung Warm Eddy, along the Offshore Branch, and at the shelf break in the southwest corner near the Korea Strait, with the organisms aggregating along the frontal zones between warm and cold water features.

We have no direct information on the types of organisms that reflected our signals. The 10-kHz acoustic pings from our instruments would reflect from swim bladders or floats of fish or siphonophores (Batzler, 1975), but they would also reflect from a high concentration of squid. Mokrin et al. (2002), referencing other sources, note that squid feed on zooplankton or nekton (myctophid fish and small juvenile squid) depending on their size; as a result, squid are more abundant in frontal-zone areas where productivity is higher. The reflective target strength of fish or squid of about 20-cm length (Urick, 1967) would require high concentrations (10^{-3} m^{-3}) such that 10^3 to 10^4 targets would contribute to the echo from a 10-kHz, 6-msec pulse at

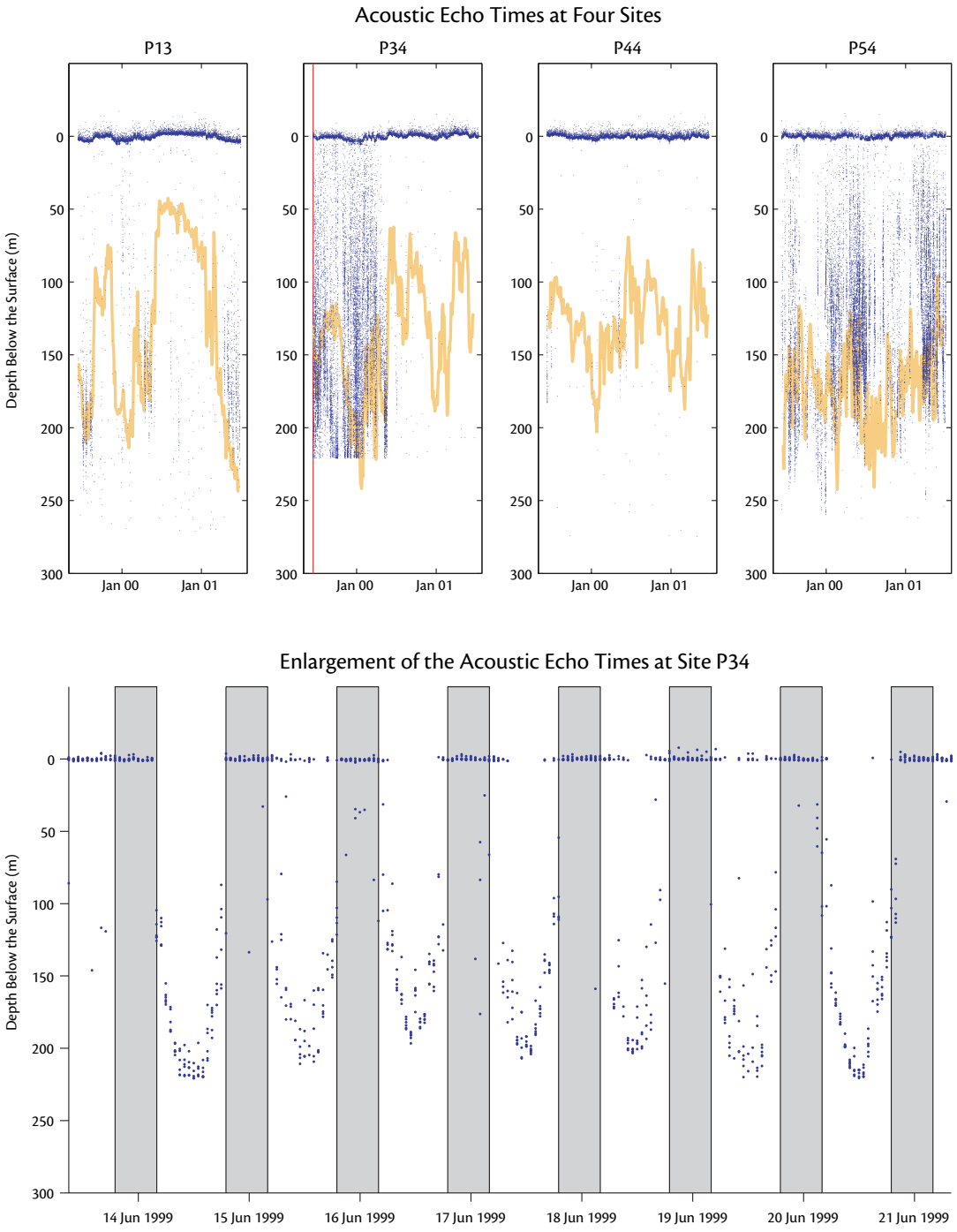

Figure 5. (Top) The blue dots show the acoustic echo returns measured at four PIES sites during June 1999 to June 2001. The desired signals are the echoes reflected off the sea surface. However, many echoes were reflected as deep as 300 m below the surface; in general, the maximum depth coincided roughly with the depth of the 5°C isotherm depth (orange line). The red bar in P34 indicates the time period, which is shown in the bottom panel. (Bottom) Acoustic echoes oscillate between the sea surface and approximately 250 m during nighttime and daylight, respectively, indicating that the echoes reflected off vertically migrating biota, such as fish or squid. Shaded bars, encompassing the hours 1900–0400 local time, indicate nighttime in the Japan/East Sea.

a range of 1000–2000 m. According to the official web site of the Ministry of Maritime Affairs and Fisheries of Korea, the amount of squid brought to the harbors located on the east coast of Korea during 1999–2001 accounted for over 50 percent of the tonnage of the total seafood catch. Approximately a billion squid are caught in the JES each year. Thus, squid is an important fishery in the JES.

Usually, fishing occurs at nighttime when bright lights attract the Japanese common squid *Todarodes pacificus* to the fishing boats. The lights on these vessels are sufficiently powerful that they can be observed from space by satellites. Cho et al. (1999) superimposed the lights from these images onto surface temperature

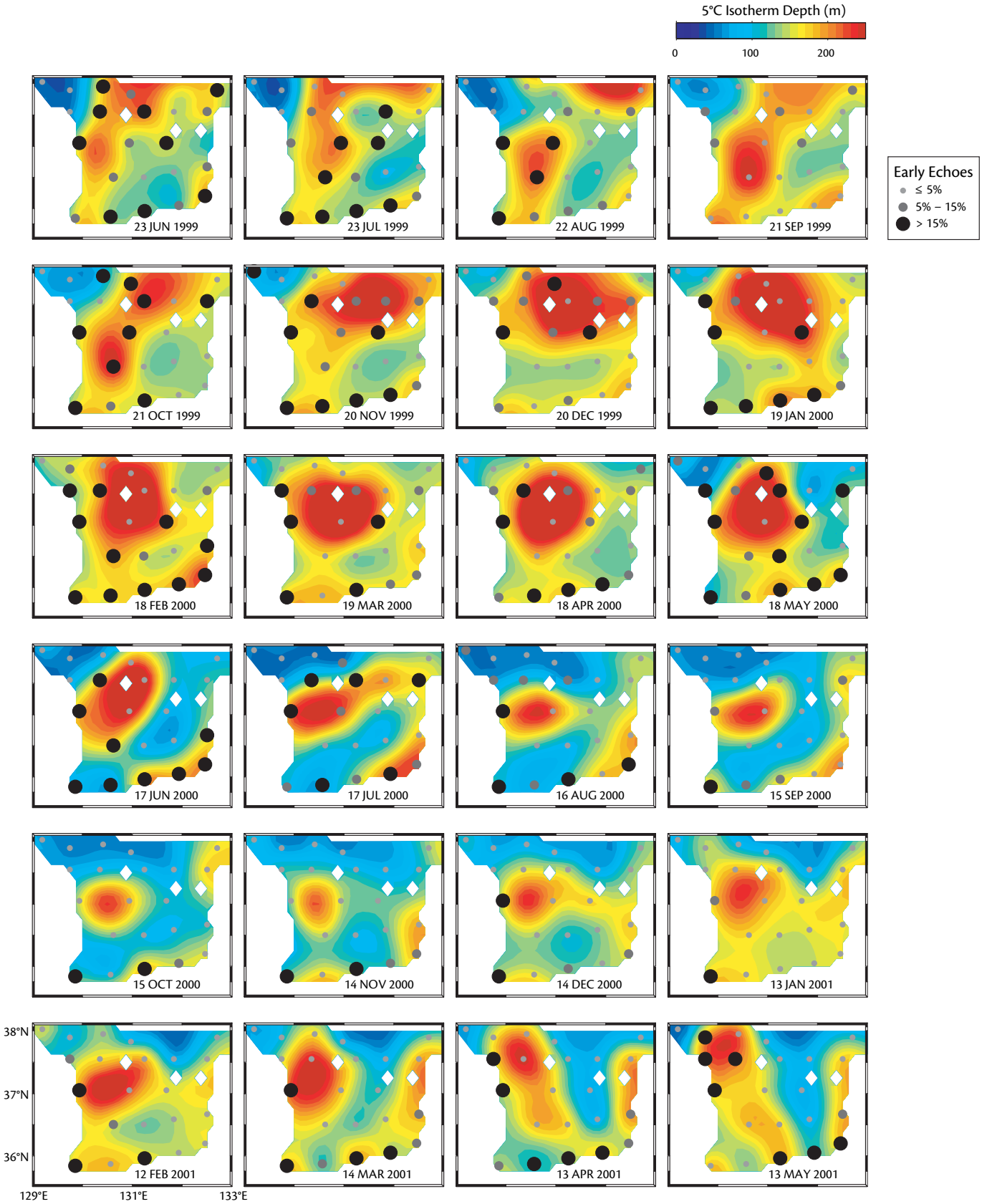

Figure 6. Maps of the 5°C isotherm depth averaged for a five-day period at 30-day intervals throughout the two-year period. The percent of early echoes received at each PIES site during each five-day period is indicated by the dots according to the key at the right. Highest percentages occur in the frontal regions between the warmer (yellow, orange, and red shaded areas) and colder waters.

maps and determined that the lights emanated from fishing vessels located along the cold side of the boundary between warm currents and cold currents. Kiyofuji and Saitoh (2004) analyzed the nighttime visible images to determine the seasonal and spatial distribution of the fishing fleet in the JES. They examined monthly composite images for the period 1994–1999, and identified seven squid fishing areas with distinct spatial and temporal occupations. They found continual fishing near the Korean and Japanese coasts and in the southwestern portion of the Ulleung Basin. On the other hand, they found fishing was essentially restricted to the month of October in the far northern regions of the JES. Their results revealed two seasonal migration routes for the squid, one along Honshu Island and the other along the Korean coast and through the central Yamato Basin. They also found an abundance of boats offshore of Korea during the second half of 1999, which coincides with our observation interval. Interestingly, their composite figures show little or no squid fishing activity in the vicinity of site P44 (near 36.5°N, 132°E), where we also observed few early echoes.

These studies suggest that the organisms responsible for our early echo reflections are either squid or the fish they are seeking as prey. Our results show that there is a strong preference for the squid to aggregate in the frontal regions between the warm and cold waters. Waluda et al. (2001) note that squid, as visual predators, would prefer the low-productivity side of frontal zones where visibility is higher. We also show that the squid descend to the depth of the thermocline as defined by the depth of the 5°C isotherm during the daytime. Thus, their spatial and temporal distribution is variable, but not simply dependent on season.

SUMMARY

In a two-year set of measurements designed to observe the upper and deep current systems in the southwestern JES, we found they differ from the "three-currents paradigm" (with seasonal modulation) that had previously existed. The upper current systems and eddies varied strongly on 50–500 day time scales. The varying circulation patterns corresponded closely with the distribution of acoustic early echoes from vertically migrating targets that likely indicate squid or fish. These animals were concentrated always near fronts between warm currents and the colder surrounding waters.

ACKNOWLEDGMENTS

This work was supported by the Office of Naval Research. M.-S. Suk was supported by grants from KORDI's in-house project (PE92700) and MOMAF's project (PM31702). K.-I. Chang was supported by the Ministry of Maritime Affairs and Fisheries, Korea (EAST-I Program) and the Research Institute of Oceanography, Seoul National University. J.-H. Yoon was supported by a grant from the Japan Marine Science Foundation under program "Study of intermediate and deep circulation of the Japan Sea."

REFERENCES

Batzler, W.E. 1975. Deep-scattering-layer observations off New Zealand and comparison with other volume scattering measurements. *Journal of the Acoustical Society of America* 58:51–71.

Chang, K.-I., N.G. Hogg, M.-S. Suk, S.-K. Byun, Y.-G. Kim, and K. Kim. 2002. Mean flow and variability in the southwestern East Sea. *Deep-Sea Research I* 49:2,261–2,279.

Chang, K.-I., W.J. Teague, S.J. Lyu, H.T. Perkins, D.-K. Lee, D.R. Watts, Y.-B. Kim, D.A. Mitchell, C.M. Lee, and K. Kim. 2004. Circulation and currents in the southwestern East/Japan Sea: Overview and review. *Progress in Oceanography* 61:105–156.

Cho, K, R. Ito, H. Shimoda, and T. Sakata. 1999. Fishing fleet lights and sea surface temperature distribution observed by DMSP/OLS sensor. *International Journal of Remote Sensing* 20:3–9.

Kiyofuji, H., and S.-I. Saitoh. 2004. Use of nighttime visible images to detect Japanese common squid *Todarodes pacificus* fishing areas and potential migration routes in the Sea of Japan. *Marine Ecology Progress Series* 276:173–186.

Lyu, S.J., and K. Kim. 2005. Subinertial to interannual transport variations in the Korea Strait and their possible mechanisms. *Journal of Geophysical Research* 110:C12016, doi: 10.1029/2004JC002651.

Lyu, S.-J., K. Kim, and H.T. Perkins. 2002. Atmospheric pressure-forced subinertial variations in transport through the Korea Strait. *Geophysical Research Letters* 29:1294, doi:10.1029/2001GL014366.

Mitchell, D. A., D.R. Watts, M. Wimbush, W.J. Teague, K.L. Tracey, J.W. Book, K.-I. Chang, M.-S. Suk, and J.-H. Yoon. 2005a. Upper circulation patterns in the Ulleung Basin. *Deep-Sea Research II* 52:1,617–1,638.

Mitchell, D.A., W.J. Teague, M. Wimbush, D.R. Watts, and G.G. Sutyrin. 2005b. The Dok Cold Eddy. *Journal of Physical Oceanography* 35:273–288.

Mokrin, N.M., Y.V. Novikov, and Y.I. Zuenko. 2002. Seasonal migrations and oceanographic conditions for concentration of the Japanese flying squid (*Todarodes pacificus* Steenstrup, 1880) in the northwestern Japan Sea. *Bulletin of Marine Science* 7:487–499.

Park, J.-H., and D.R. Watts. 2005. Response of the southwestern Japan/East Sea to atmospheric pressure. *Deep-Sea Research II* 52:1,671–1,683.

Park, J.-H., and D.R. Watts. 2006. Internal tides in the southwestern Japan/East Sea. *Journal of Physical Oceanography* 36:22–34.

Teague, W.J., G.A. Jacobs, D.A. Mitchell, M. Wimbush, and D.R. Watts. 2004. Decadal current variations in the southwestern Japan/East Sea. *Journal of Oceanography* 60:1,023–1,033.

Teague, W.J., K.L. Tracey, D.R. Watts, J.W. Book, K.-I. Chang, P.J. Hogan, D.A. Mitchell, M.-S. Suk, M. Wimbush, and J.-H. Yoon. 2005. Observed deep circulation in the Ulleung Basin. *Deep-Sea Research II* 52:1,802–1,826.

Urick, R.J. 1967. *Principles of Underwater Sound for Engineers*. McGraw-Hill, 342 pp.

Waluda, C.M., P.G. Rodhouse, P.N. Trathan, and G.J. Pierce. 2001. Remotely sensed mesoscale oceanography and the distribution of *Illex argentinus* in the South Atlantic. *Fisheries Oceanography* 10:207–216.